AIAA JOURNAL
Vol. 33, No. 11, November 1995

Using Transfer Function Parameter Changes for Damage Detection of Structures

Jiann-Shiun Lew*
Tennessee State University, Nashville, Tennessee 37203

A novel approach is presented for damage detection of large flexible structures by using the parameter change of the transfer function. First, an interval modeling technique, which represents the system uncertainty under the environmental change via the intervals of transfer function parameters, is used to distinguish the structural damage from the environmental change. In this paper a coherence approach is developed for locating the damage position when the structural damage is observed. Only a few sensors are required in using the proposed coherence approach for damage detection. This has the advantage of using the proposed algorithm for practical applications. Also this approach has the flexibility of using the multi-input and multi-output system. A nine-bay truss example is used to demonstrate and verify the approach developed.

Nomenclature

a, b	= denominator and numerator parameters of transfer function
C	= coherence of the tested system to damage
G	= interval model
g	= transfer function
k	= number of modes
m	= number of outputs
n	= number of tests for environmental change
$\boldsymbol{p}$	= parameter vector of transfer function
R	= magnitude ratio of the tested system to damage
$\bar{R}, \underline{R}$	= magnitude ratio bounds
W	= weight of parameter change
W_a, W_b	= weights of intervals for interval model
$\hat{x}, \hat{y}$	= unit vectors of Cartesian coordinate system
$\Delta\boldsymbol{p}$	= parameter change vector

Superscripts

W	= weighted parameter change
$-, +$	= lower and upper bounds

Introduction

THE operation of large flexible space structures is sensitive to the damage of the structural components. To maintain the performance and safe operation of the system, it is necessary to remotely monitor the mechanical health of the structure. Then the control systems and adaptive components can respond to improve mission performance.

The identified model of a system is varied with the environmental change and the structural damage. The first step of damage detection is to identify the status of the system damage. In this paper, an interval modeling technique, which represents the system with uncertainty via a model set whose transfer function coefficients are bounded,[1,2] is used to quantify the system parametric uncertainty due to the environmental change. This approach initially obtains the system identified models under the environmental change by running many tests, e.g., Monte Carlo runs, under different circumstances. One can then use these identified models to generate an interval model to represent the system with the environmental change. The status of system damage is determined by checking whether the parameter change of the tested system is outside the interval model. If system damage is observed, one may carry the analysis forward to detect the damage location.

Recently different approaches for damage location and estimation have been proposed.[3-5] Most of them are based on the finite element model (FEM) update techniques. These techniques are based on the parameter changes of the stiffness and mass matrices between the damaged system and undamaged system. In general, these methods require a large number of sensors to measure mode shapes accurately. But the number of sensors is limited in practical applications. Also researchers have shown that these methods can generate ambiguous results unless the modes with high-strain energy are used.[3] Recently neural network techniques have been applied to structural damage detection.[6,7] The neural network approach uses the patterns from the past experience to detect system damage and, thus, requires the data of the previous patterns. The neural network approach is a learning process and does not provide information about system parameter changes. In general, the neural network approach does not provide for theoretical analysis.

This paper presents a novel approach to locate the damage position based on the comparison of the transfer function parameter change of the tested system and the change due to damage. Unlike most other damage detection approaches, which use finite element model update techniques, the proposed approach considers the parameter change of the transfer function. The approach is based on the fact that the system transfer function parameter change due to damage is uniquely determined by the damage type and location. The coherence between the parameter change of the tested system and the change due to damage is used to locate the damage position. Only a few sensors are required for this approach. Also the proposed approach has the flexibility of using the multi-input and multi-output system.

Damage Detection Approach

In this damage detection approach, we first use an interval modeling technique to quantify the environmental change. The identified interval model is used to determine the damage status of the tested system. If system damage is observed, a coherence algorithm is used to locate the damage position.

Interval Modeling Technique

To present this interval modeling technique simply, we use a single-input and single-output system. Here we consider n sets of experimental data of the healthy structure from n tests under environmental changes. The experimental data can be time-domain response data or frequency-domain response data. We apply system identification algorithms[8-10] to process each of the n sets of experimental data to obtain the identified transfer functions[2]

Received Feb. 21, 1995; revision received May 30, 1995; accepted for publication June 2, 1995.

*Research Professor, Center of Excellence in Information Systems and Center for Automated Space Science. Member AIAA.

$$g_i(s) = \frac{b_l^i s^l + b_{l-1}^i s^{l-1} + \cdots + b_0^i}{s^l + a_{l-1}^i s^{l-1} + \cdots + a_0^i}$$

$$= b_i + \sum_{j=1}^{k} \frac{b_{ij1} s + b_{ij0}}{s^2 + a_{ij1} s + a_{ij0}} \qquad i = 1, \ldots, n \tag{1}$$

where b_j^i and a_j^i are numerator and denominator coefficients of the identified model of the ith test, respectively. The variables b_i, b_{ijk}, and a_{ijk} are the corresponding parameters of the ith identified transfer function with second-order form. After the identified models of all of the tests are obtained, an interval model[1] is generated:

$$G(s, p) = \left\{ b + \sum_{j=1}^{k} \frac{b_{1j} s + b_{0j}}{s^2 + a_{1j} s + a_{0j}} : \quad b \in [b^- \quad b^+] \right.$$
$$\left. b_{lj} \in \left[b_{lj}^- \quad b_{lj}^+\right], a_{lj} \in \left[a_{lj}^- \quad a_{lj}^+\right] \right\} \tag{2}$$

where the interval bounds of each parameter are chosen as the maximum and minimum of the corresponding identified parameters of all the tests[11]; for example,

$$b^+ = \max\{b_1, b_2, \ldots, b_n\} \tag{3}$$

Later examples will be used to demonstrate how to use this interval modeling technique to quantify the environmental change. The procedures to decide which damage cases can be distinguished from the environmental change also will be discussed.

Coherence Approach

The coherence approach is based on the fact that the change of the system transfer function is uniquely determined by the system damage type and location. To concisely present this approach, we consider the model of the selected k modes for a structure with m displacement outputs and single input. Here we consider the analytical models, which are obtained by applying finite element analysis, with zero damping. The transfer functions of these m outputs of the healthy structure are

$$g_{0j} = \sum_{l=1}^{k} \frac{b_{0jl}}{s^2 + a_{0l}}, \qquad j = 1, \ldots, m \tag{4}$$

where a_{0l} and b_{0jl} are the parameters of the lth modes of the jth output. Because natural frequencies are system characteristics, the lth modes of all of the outputs share the same variable a_{0l}, which is the square of the lth natural frequency. Here we define the parameter vectors of the healthy structure as

$$\boldsymbol{p}_{00} = [a_{01} \quad a_{02} \quad \cdots \quad a_{0k}]^T$$
$$\boldsymbol{p}_{0j} = [b_{0j1} \quad b_{0j2} \quad \cdots \quad b_{0jk}]^T, \qquad j = 1, \ldots, m \tag{5}$$

where the lth elements of $\boldsymbol{p}_{00}$ is the square of the lth natural frequency, and the lth element of $\boldsymbol{p}_{0j}$ is the numerator coefficient of the lth mode for the jth output. The transfer functions of the system with the ith element damage are expressed as

$$g_{ij} = \sum_{l=1}^{k} \frac{b_{ijl}}{s^2 + a_{il}}, \qquad j = 1, \ldots, m \tag{6}$$

where the indexes i, j, and l represent the numbers of damage element, output, and mode, respectively. The corresponding parameter vectors of the system with ith element damage are defined as

$$\boldsymbol{p}_{i0} = [a_{i1} \quad a_{i2} \quad \cdots \quad a_{ik}]^T$$
$$\boldsymbol{p}_{ij} = [b_{ij1} \quad b_{ij2} \quad \cdots \quad b_{ijk}]^T, \qquad j = 1, \ldots, m \tag{7}$$

The changes of the parameter vectors due to the damage of the ith element are

$$\Delta \boldsymbol{p}_{ij} = \boldsymbol{p}_{ij} - \boldsymbol{p}_{0j}, \qquad j = 0, 1, \ldots, m \tag{8}$$

Because of the perturbation of each parameter, we define the weighted parameter change vectors as

$$\Delta \boldsymbol{p}_{ij}^W = [\Delta \boldsymbol{p}_{ij}(1)/W_{j1} \quad \Delta \boldsymbol{p}_{ij}(2)/W_{j2} \cdots \Delta \boldsymbol{p}_{ij}(k)/W_{jk}]^T \tag{9}$$

where $\Delta \boldsymbol{p}_{ij}(l)$ is the lth element of $\Delta \boldsymbol{p}_{ij}$ and W_{jl} is the mean square root of $\{\Delta \boldsymbol{p}_{1j}(l), \Delta \boldsymbol{p}_{2j}(l), \ldots, \Delta \boldsymbol{p}_{nj}(l)\}$. The weight W_{jl} is the mean square root of the numerator coefficient change of the lth mode of the jth output due to all of the damage cases. Consider the tested system with the weighted parameter change vectors $\Delta \boldsymbol{p}_j^W$, $j = 0, \ldots, m$. The coherences between the change vectors $\Delta \boldsymbol{p}_j^W$ of the tested system and the change vectors $\Delta \boldsymbol{p}_{ij}^W$ of the ith damage case are defined as

$$C_{ij} = \frac{\left(\Delta \boldsymbol{p}_j^W\right)^T \Delta \boldsymbol{p}_{ij}^W}{\left|\Delta \boldsymbol{p}_j^W\right| \left|\Delta \boldsymbol{p}_{ij}^W\right|}, \qquad j = 0, 1, \ldots, m \tag{10}$$

The variables C_{ij}, $j = 0, 1, \ldots, m$, represent the coherences of directions of the parameter change vectors between the tested system and the system with the ith element damage for the chosen m outputs. Here we define the minimum coherence of the tested system corresponding to the ith damage case as

$$C_i = \min\{C_{i0}, C_{i1}, \ldots, C_{im}\} \tag{11}$$

The magnitude ratios between the parameter change vectors $\Delta \boldsymbol{p}_j^W$ of the tested system and the parameter change vectors $\Delta \boldsymbol{p}_{ij}^W$ due to the ith element damage are defined as

$$R_{ij} = \frac{\left|\Delta \boldsymbol{p}_j^W\right|}{\left|\Delta \boldsymbol{p}_{ij}^W\right|}, \qquad j = 0, 1, \ldots, m \tag{12}$$

Here we also define the magnitude ratio bounds of the tested system corresponding to the ith damage case as

$$\bar{R}_i = \max\{R_{i0}, R_{i1}, \ldots, R_{im}\} \tag{13}$$

$$\underline{R}_i = \min\{R_{i0}, R_{i1}, \ldots, R_{im}\} \tag{14}$$

Some properties associated with C_{ij}, C_i, R_{ij}, $\bar{R}_i$, and $\underline{R}_i$ are as follows:

1) When both C_{ij} and R_{ij} ($j \geq 1$) are equal to 1, the parameter change vector $\boldsymbol{p}_j^W$ is in the same direction and has the same magnitude as the parameter change vector $\boldsymbol{p}_{ij}^W$ of the jth output due to the ith element damage.

2) If the tested system is the system with the ith element damaged, all of these variables are equal to 1.

3) The variable C_{ij} is between -1 and 1. When C_{ij} is less than 0, the change of the numerator parameter vector of the jth output of the tested system is in the different direction ($\geq$90 deg) from the change due to the ith element damage. It strongly infers that the ith element is not damaged.

4) The magnitude ratio bounds $\bar{R}_i$ and $\underline{R}_i$ represent the relationship of the magnitude of the parameter change between the tested system and the system with ith element damage. If the tested system is the system with the ith element damage, both $\bar{R}_i$ and $\underline{R}_i$ are equal to 1. If $\bar{R}_i / \underline{R}_i \gg 1$ or both $\bar{R}_i$ and $\underline{R}_i$ are far away from 1, it strongly infers that the ith element is not damaged.

Here the coherence approach for the single-input system is presented. This approach can also be applied to the multi-input system.

Example

The finite element model[12] of a nine-bay truss structure as shown in Fig. 1 is chosen as the system for the numerical study. This structure is cantilevered to the ground at the end. The structure has 9 bays with 45 bar elements, and each nondiagonal element is a 3-m-long aluminum tube with cross-sectional area of 1.382×10^{-4} m^2. First, a study of the coherence algorithm based on the model of the modes with natural frequencies below 100 Hz is presented. There are four modes below 100 Hz and the natural frequencies of these modes are 4.986, 27.717, 39.787, and 67.434 Hz, respectively.

In the study of the coherence algorithm, we use the FEM model of the system with one input at node 20 and four displacement outputs

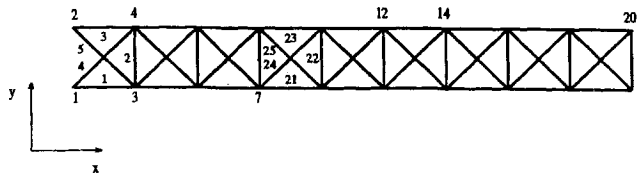

Fig. 1 Nine-bay truss structure.

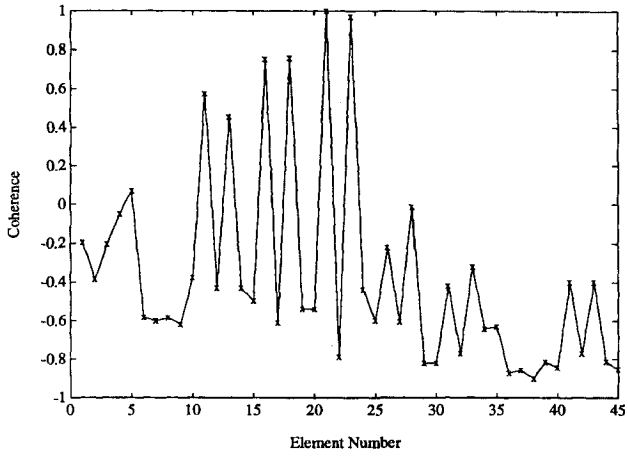

Fig. 2 Minimum coherence C_i for the beam 21 damage case with input in $\hat{y}$ direction.

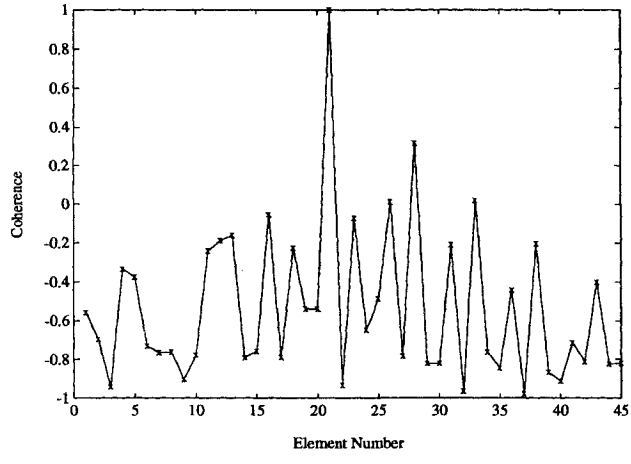

Fig. 3 Minimum coherence C_i for the beam 21 damage case with input in $\hat{x} + 2\hat{y}$ direction.

at nodes 20, 14, 12, and 7. All of the outputs are in the $\hat{y}$ direction. For the system damage, a beam is removed for each case. Here we present two cases with beam 21 or 25 removed, respectively. Figures 2 and 3 show the results of the minimum coherences C_i for the beam 21 damage when the inputs with different directions are used. These inputs are in the $\hat{y}$ direction and in the $\hat{x} + 2\hat{y}$ direction, respectively. Because of the symmetry of this nine-bay truss structure, the transfer function change due to the damage of beam 21 and the change due to the damage of beam 23 are very close when the input is in the $\hat{y}$ direction. Figure 2 shows that both of the minimum coherences C_{21} and C_{23} are close to 1. Figure 3 shows that using input in the $\hat{x} + 2\hat{y}$ direction can significantly improve the problem due to the symmetry of the structure, and the damage position is well identified. In Fig. 3, the largest coherence is C_{21} with a value of 1, and the second largest coherence is C_{28} with a value of 0.316. The following discussions are based on the results with input in the $\hat{x} + 2\hat{y}$ direction. Figure 4 shows the results of the minimum coherences C_i for beam 25 damage and the damage position is well identified. To demonstrate the effect of using the responses from more than one input, we choose a system with two inputs at nodes 15 and 20. Here we add the responses with the input in the $-\hat{x} + 2\hat{y}$ direction at node 15. In Fig. 5, x represents the previous results of the system with one input and o represents

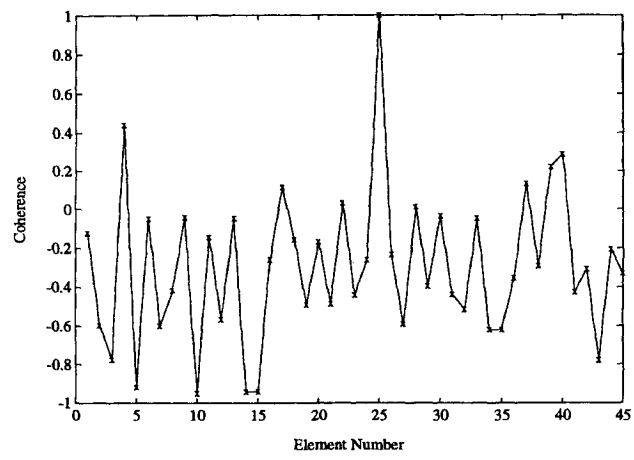

Fig. 4 Minimum coherence C_i for the beam 25 damage case.

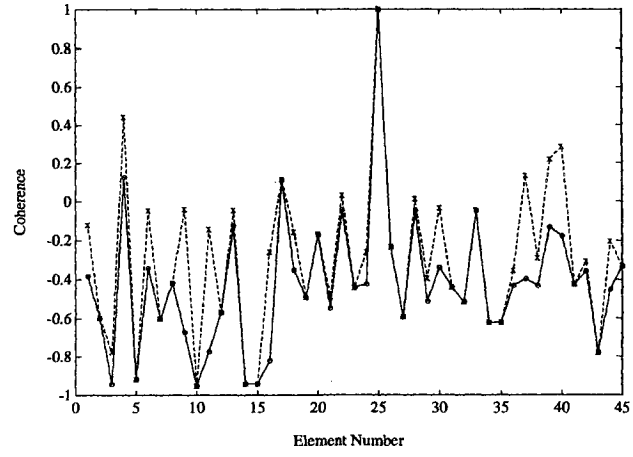

Fig. 5 Minimum coherence C_i for the beam 25 damage case: x one input, o two inputs.

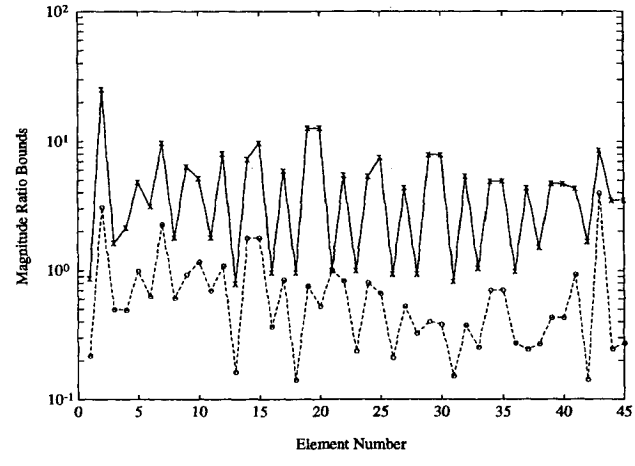

Fig. 6 Magnitude ratio bounds for the beam 21 damage case: x upper bound, o lower bound.

the results of the system with two inputs. For the single-input case, eight minimum coherences are positive, and the second largest is 0.443. For the case with two inputs, the number of positive minimum coherences is reduced to 3, and the second largest is 0.127. This demonstrates the improvement by using the responses from the multi-input system. The results of the magnitude ratio bounds for the case with beam 21 damage are shown in Fig. 6. The maximum magnitude ratios $\bar{R}_i$ are about one order larger than the minimum magnitude ratios $\underline{R}_i$ except that $\bar{R}_{21}$ and $\underline{R}_{21}$ are equal to 1. These magnitude ratio bounds are additional good references for locating damage position.

Next we discuss the results of applying the interval modeling technique to model the identified parameter change under the

environmental change. Here we consider the model of the first two modes of the system with one input in the $\hat{x} + 2\hat{y}$ direction at node 20 and one displacement output in the $\hat{y}$ direction at node 20. The transfer function of the FEM model of this system is

$$g(s) = \frac{2.8310 \times 10^{-1}}{s^2 + 9.8155 \times 10^2} + \frac{1.8953 \times 10^{-1}}{s^2 + 3.0328 \times 10^4}$$

In this part of the study, there are 15 sets of noisy pulse response data used to represent the system undergoing environmental change. The noise is modeled as additive, white, and Gaussian, and its magnitude is 5% of the magnitude of the pulse response data. We apply ERA/DC[8,9] system identification algorithm to process each set of the noisy pulse response data to obtain the identified models. These models are used to generate an interval model with the form

$$G(s, p) = \left\{ \sum_{i=1}^{2} \frac{b_{0i}}{s^2 + a_{0i}}: \quad b_{0i} \in \left[b_{0i}^- \; b_{0i}^+\right], \; a_{0i} \in \left[a_{0i}^- \quad a_{0i}^+\right] \right\} \tag{15}$$

For comparison, we define the weighting of the interval of each parameter as

$$W_a^i = a_{0i}^+ - a_{0i}^-, \qquad W_b^i = b_{0i}^+ - b_{0i}^- \tag{16}$$

and we normalize the intervals as

$$a_i^{\pm} = \frac{a_{0i}^{\pm} - a_{0i}^0}{W_a^i}, \qquad b_i^{\pm} = \frac{b_{0i}^{\pm} - b_{0i}^0}{W_b^i} \tag{17}$$

where a_{0i}^0 and b_{0i}^0 are the mean values of the corresponding identified parameters. Table 1 shows the results of the interval model.

Here we consider three cases with beam 21, 22, or 25 damaged, respectively. The ERA/DC algorithm is used to process the noisy pulse response data of the damage cases of this single-input and single-output system. The weighted parameter differences between the tested system and the healthy system are defined as

$$a_i^W = \frac{a_i - a_{0i}^0}{W_a^i}, \qquad b_i^W = \frac{b_i - b_{0i}^0}{W_b^i} \tag{18}$$

where the variables a_i and b_i are the identified parameters of the tested system. Table 2 shows the results of these three damage cases.

Table 2 also shows the results of a_i^W and b_i^W computed by using the parameters a_i and b_i of the finite element model and the identified parameters a_{0i}^0 and b_{0i}^0. Figure 7 shows the results of $|a_i^W|$, which are obtained by using the finite element parameters a_i and b_i, for all

Table 1 Results of interval model

	a_{0i}^-	a_{0i}^+	b_{0i}^-	b_{0i}^+
$i = 1$	9.8152e02	9.8165e02	2.8139e−1	2.8446e−1
$i = 2$	3.0323e04	3.0331e04	1.8195e−1	2.0723e−1
	a_i^-	a_i^+	b_i^-	b_i^+
$i = 1$	−0.4602	0.5398	−0.5401	0.4599
$i = 2$	−0.3916	0.6084	−0.4169	0.5831

Table 2 Weighted parameter differences

Damage	a_1^W	a_2^W	b_1^W	b_2^W
		ID model		
Beam 21	−1.5333e03	−1.7056e03	1.1383e01	−1.4119e00
Beam 22	2.1667e02	3.0963e02	2.8194e00	−4.6420e−1
Beam 25	4.5387e01	2.4588e02	1.4052e00	6.4050e−2
		FEM model		
Beam 21	−1.5334e03	−1.7054e03	1.0638e01	−1.8276e00
Beam 22	2.1664e02	3.1042e02	2.8957e00	−4.6346e−1
Beam 25	4.5101e01	2.4559e02	1.1055e00	−2.0862e−1

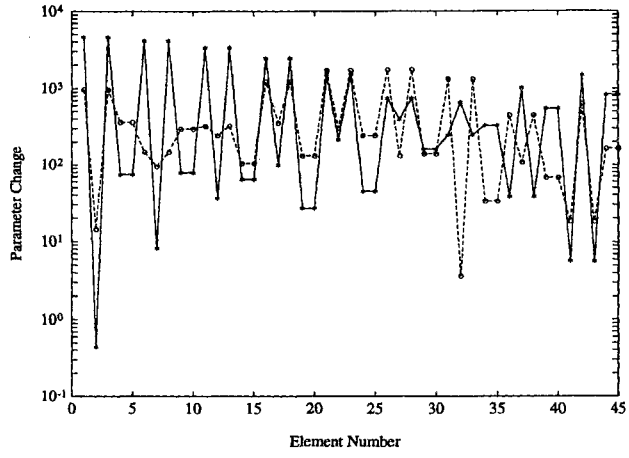

Fig. 7 Weighted parameter change for all of the damage cases: x $|a_1^W|$, o $|a_2^W|$.

of the damage cases. From the results, the following observations are noted.

1) Table 1 shows that the natural frequencies, which are the square root of a_{0i}, are affected little by the assumed environmental change. When the system is damaged, the system characteristics change dramatically, so the variables a_i, which are the squares of natural frequencies, change significantly. In Table 2, the variables a_i^W due to the system damage are around 10^2–10^3 times larger than the interval bounds $a_i^{\pm}$ of the environmental change. Using the variables a_i^W and the interval bounds $a_i^{\pm}$, the system damage can be distinguished from the environmental change for these three damage cases. The variables a_i^W obtained by using the parameters of the finite element model are almost exactly the same as that obtained by using system identification parameters because the variables a_i^W are not sensitive to the assumed environmental change.

2) Table 1 shows that the identified numerator parameters are much more sensitive to the environmental change than the identified denominator parameters. From Table 2, the variables b_i^W due to the damage of beam 22 or 25 have magnitudes similar to the interval bounds $b_i^{\pm}$ of the environmental change. The variables b_i^W are not as reliable for distinguishing the system damage from the environmental change as the variables a_i^W.

3) Figure 7 shows the results of $|a_i^W|$ for all of the damage cases. Most of the variables $|a_i^W|$ are about 10^2–10^3 times larger than the interval length of the environmental change. For the beam 2 damage case, the variable $|a_1^W|$ is smaller than 1, but $|a_2^W|$ is larger than 10 and so this damage case is clearly distinguished from the environmental change. All of the damage cases can be distinguished from the environmental change by using the variables $|a_i^W|$.

The procedures to check whether the damage case can be distinguished from the environmental change are as follows.

1) Obtain the identified models of various tests that represent the system under the environmental change.

2) Use the identified models to generate an interval model.

3) Use the parameters a_i and b_i of the finite element model of the damage case to obtain variables a_i^W and b_i^W.

4) Check whether any one of these variables has a magnitude level larger than 1: a) yes, this damage can be distinguished or b) no, this damage cannot be distinguished.

For the real system, some system damages may not be distinguished from the environmental change. Following the given procedures, we can decide which damage cases can be distinguished from the environmental change. All of the damage cases in this example can be distinguished from the assumed environmental change by using the preceding process. After the system damage is detected, the next step is to locate the damage position by applying the developed coherence algorithm. Here we consider the model of the first two modes of the preceding system with one input and four displacement outputs. The ERA/DC algorithm is used to process the noisy pulse response data of the healthy structure and the tested system with beam 21 damage to obtain the identified models. The

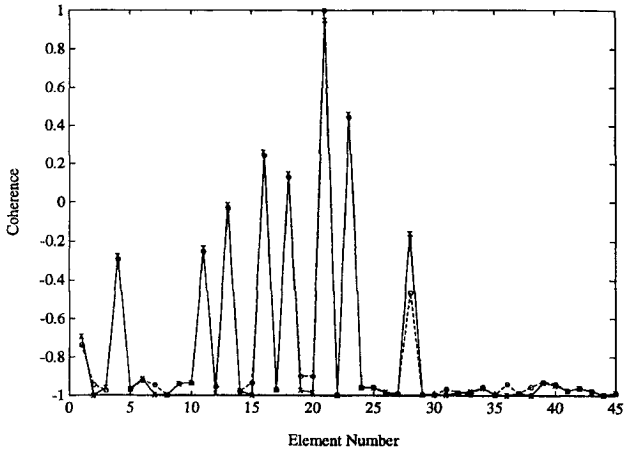

Fig. 8 Minimum coherence C_i for the beam 21 damage case: x identified model, o finite element model.

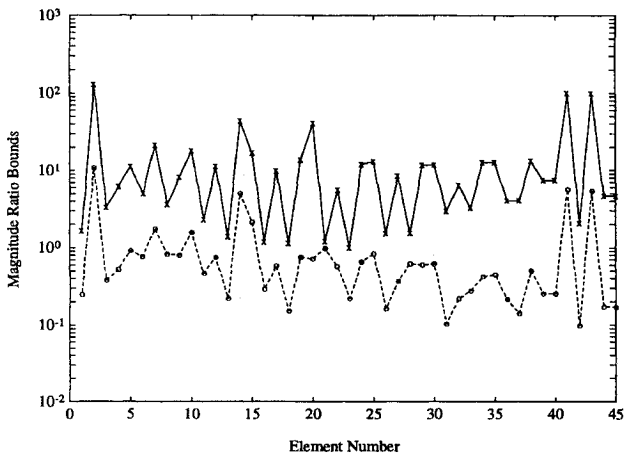

Fig. 9 Magnitude ratio bounds for the beam 21 damage case: x upper bound, o lower bound.

magnitude of the noise is 5% of the magnitude of the pulse response for each output. The changes of the parameter vectors [see Eq. (8)] of the tested system are defined as

$$\Delta \boldsymbol{p}_j^0 = \boldsymbol{p}_j^0 - \boldsymbol{p}_{0j}^0, \qquad j = 0, 1, 2, 3, 4 \tag{19}$$

where $\boldsymbol{p}_j^0$ and $\boldsymbol{p}_{0j}^0$ are the identified parameter vectors of the tested system and healthy structure, respectively. The vectors $\Delta \boldsymbol{p}_j^0$ of the identified models and the vectors $\Delta \boldsymbol{p}_{ij}$ of the finite element models are used to obtain the coherences of this tested system. In Fig. 8, x represents the minimum coherences based on the analysis of the parameter vectors $\Delta \boldsymbol{p}_j^0$ and o represents the minimum coherences based on the analysis of the parameter vectors $\Delta \boldsymbol{p}_j$ of the finite element model for the system with beam 21 damage. Also the bounds of the magnitude ratios are shown in Fig. 9. From Figs. 8 and 9, the following observations are noted.

1) The minimum coherences C_i of the system with uncertainty, which is represented as the added noise, are close to that of the system without uncertainty. The minimum coherences obtained by analyzing the noisy pulse response data well identify the damage location.

2) Both of the magnitude ratio bounds $\bar{R}_{21}$ and $\underline{R}_{21}$ are very close to 1 for the system with uncertainty. They can be used as the reference to identify the damage location.

Concluding Remarks

A novel approach is presented for damage detection of large structures. First, an interval modeling technique is used to quantify the parameter change due to environmental change. The results show that the system's natural frequencies change little due to the environmental change, but they change dramatically due to the system damage. The changes of the natural frequencies can be used to distinguish system damage from environmental change.

In this paper, a coherence algorithm is used to locate the damaged position if the system damage is detected. This approach is based on the fact that the transfer function change due to damage is uniquely determined by the damage type and location. Only a few sensors are required in using the proposed approach. The results based on the analysis of the noisy response data show that this coherence algorithm well identifies the damaged element when the system has uncertainty. In addition, the bounds of magnitude ratios are reliable references for distinguishing the damaged element. The developed coherence approach can also be applied to the multi-input and multi-output system. Using the multi-input and multi-output system can improve the performance of the coherence algorithm.

Acknowledgments

This research is supported in part by NASA Grant NCCW-0085 and NASA Grant NAG 5-2109. These supports are greatly appreciated.

References

[1]Lew, J.-S., Keel, L. H., and Juang, J.-N., "Quantification of Parametric Uncertainty via an Interval Model," *Journal of Guidance, Control, and Dynamics*, Vol. 17, No. 6, 1994, pp. 1212–1218.

[2]Lew, J.-S., Link, T., Garcia, E., and Keel, L. H., "Interval Model identification for Flexible Structures with Uncertain Parameters," *Proceedings of the AIAA/ASME Adaptive Structures Forum*, AIAA, Washington, DC, 1994, pp. 42–48.

[3]Peterson, L. D., Alvin, K. F., Doebling, S. W., and Park, K. C., "Damage Detection Using Experimentally Measured Mass and Stiffness Matrices," *Proceedings of the AIAA/ASME/AHS/ASC 34th Structures, Structural Dynamics, and Materials Conference*, AIAA, Washington, DC, 1993, pp. 1518–1528.

[4]Zimmerman, D. C., and Kaouk, M., "Structural Damage Detection Using a Subspace Rotation Algorithm," *Proceedings of the AIAA/ASME/AHS/ASC 33rd Structures, Structural Dynamics, and Materials Conference*, AIAA, Washington, DC, 1992, pp. 2341–2350.

[5]Pandey, A. K., Biswas, M., and Samman, M., "Damage Detection from Changes in Curvature Mode Shapes," *Journal of Sound and Vibration*, Vol. 145, No. 2, 1991, pp. 321–332.

[6]Tsou, P., and Shen, M.-H., "Structural Damage Detection and Identification Using Neural Network," *Proceedings of the AIAA/ASME/AHS/ASC 34th Structures, Structural Dynamics, and Materials Conference*, AIAA, Washington, DC, 1993, pp. 3551–3560.

[7]Povich, C. R., and Lim, T. W., "An Artificial Neural Network Approach to Structural Damage Detection Using Frequency Response Functions," *Proceedings of the AIAA/ASME Adaptive Structures Forum*, AIAA, Washington, DC, 1994, pp. 151–159.

[8]Juang, J.-N., Phan, M., and Horta, L. G., "User's Guide for System/Observer/Controller Identification Toolbox," NASA TM 107566, 1992.

[9]Lew, J.-S., Juang, J.-N., and Longman, R. W., "Comparison of Several System Identification Methods for Flexible Structures," *Journal of Sound and Vibration*, Vol. 167, No. 3 , 1993, pp. 461–480.

[10]Bayard, D. S., Hadaegh, F. Y., Yam, Y., Scheid, R. E., Mettler, E., and Milman, M. H., "Automated On-Orbit Frequency Domain Identification for Large Space Structures," *Automatica*, Vol. 27, No. 11, 1991, pp. 931–946.

[11]Lew, J.-S., "Using Transfer Function Parameter Changes for Damage Detection of Structures," *Proceedings of the AIAA/ASME/AHS/ASC 36th Structures, Structural Dynamics, and Materials Conference and AIAA/ASME Adaptive Structures Forum*, AIAA, Washington, DC, 1995, pp. 2893–2900.

[12]Craig, R. R., *Structural Dynamics: An Introduction to Computer Methods*, Wiley, New York, 1981.